Original Article

Down-regulation of LCN2 attenuates retinal vascular dysfunction and caspase-1-mediated pyroptosis in diabetes mellitus

Xingjie Su[#], Pingping Zhou[#], Yanxiu Qi

Department of Ophthalmology, The First Affiliated Hospital of Jiamusi University, Jiamusi, China

Contributions: (I) Conception and design: X Su; (II) Administrative support: Y Qi; (III) Provision of study materials or patients: X Su; (IV) Collection and assembly of data: X Su, P Zhou; (V) Data analysis and interpretation: P Zhou; (VI) Manuscript writing: All authors; (VII) Final approval of manuscript: All authors.

[#]These authors contributed equally to this work.

Correspondence to: Yanxiu Qi. Department of Ophthalmology, The First Affiliated Hospital of Jiamusi University, 348 Dexiang Street, Jiamusi 154002, China. Email: suyunyi1998@sina.com

Background: Diabetic retinopathy (DR) is a diabetic microangiopathy with increasing incidence, which seriously threatens the quality of life of patients. This study investigated the molecular regulation mechanism of lipocalin-2 (LCN2) in DR by targeting the function of human retinal vascular endothelial cells (HRVECs).

Methods: The expression of LCN2 in the retinal tissue of diabetic and high glucose (HG)-induced HRVECs was detected by reverse transcription quantitative polymerase chain reaction (RT-qPCR) analysis and western blotting assay. After intravitreal injection of adeno-associated virus (AAV)-NC or AAV-sh-LCN2, *in vivo* experiments, hematoxylin and eosin (H&E) staining, and retinal trypsin digestion experiments were performed to analyze the effect of LCN2 silencing on DR retinal tissue. Terminal deoxynucleotidyl transferase biotin-dUTP nick end labeling (TUNEL) staining was used to evaluate apoptosis and immunohistochemical (IHC) staining was performed to detect the expressions of caspase-1. Western blot was used to detect the expressions of pyroptosis-associated proteins. After transfection of sh-NC and sh-LCN2, the function of HRVECs cells induced by HG was evaluated by wound healing assay, Transwell assay, and tube formation assay.

Results: The expression of LCN2 was significantly up-regulated in diabetic retinal tissue and HG-induced HRVECs. *In vivo* experiments showed that LCN2 silencing can significantly reduce diabetic retinal injury. Cell function experiments also revealed that LCN2 silencing inhibited cell migration, invasion, and angiogenesis. Flow cytometry and immunofluorescence staining showed that downregulation of LCN2 could inhibit caspase-1 mediated pyroptosis in HG-induced HRVECs.

Conclusions: Down-regulation of LCN2 can significantly inhibit cell migration, invasion, and angiopoiesis, and pyroptosis regulated by caspase-1, thus attenuating the progression of DR.

Keywords: Lipocalin-2 (LCN2); pyroptosis; human retinal vascular endothelial cells (HRVECs); diabetic retinopathy (DR)

Submitted Apr 29, 2022. Accepted for publication Jun 20, 2022.
doi: 10.21037/atm-22-2655
View this article at: https://dx.doi.org/10.21037/atm-22-2655

Introduction

Diabetic retinopathy (DR) is one of the most common complications of diabetes. It is caused by microvascular injury and is currently a key cause of blindness in patients (1,2). The incidence of DR has increased dramatically over the past few decades. Some studies have predicted that the case number of DR will approach 200 million by 2030 (3). Currently, the known pathological mechanism of DR mainly involves oxidative stress induced by a

continuous high glucose (HG) environment (4), abnormal vascular permeability, microvascular aneurysm (5), vascular obstruction, and endothelial cell dysfunction (6). Due to the complex pathological mechanism of DR, effective treatment strategies and drugs are very limited. It is necessary to further study the molecular mechanism of DR in order to accurately predict and effectively develop specific treatment plans.

It has been reported (7) that retinal endothelial cell death is a key step in the progression of DR, in which apoptosis, necrosis, autophagy, and pyroptosis have been identified as the death mechanisms. Apoptosis (8) and autophagy (9) have been thoroughly studied and confirmed in DR. However, whether scoria of human retinal vascular endothelial cells (HRVECs) is related to the development of DR has rarely been reported. Pyroptosis is commonly thought to be caspase-1-dependent apoptosis activated by the inflammatory cytokine interleukin (IL)-1β (10). Further research on pyroptosis of retinal endothelial cells may provide new therapeutic strategies for DR therapy.

It is well known that lipocalin-2 (LCN2) is a neutrophil gelatinase-associated lipid calin (NGAL), which is mainly secreted by hepatocytes (11). It is a secretory glycoprotein in the lipid transporter superfamily that is involved in regulating various cellular functions such as migration (12), inflammatory cytokine release, and apoptosis. It has been reported (13) that LCN2 plays an important role in the pathogenesis of ischemic stroke, especially in the regulation of the inflammatory response. In addition, LCN2 is also abnormally expressed in various cancers, affecting the malignant progression of cervical cancer (14), colorectal cancer (15), and breast cancer (16). Xu *et al.* (17) reported that LCN2 could specifically bind to *SLPI* to promote the proliferation, invasion, and metastasis of gastric cancer cells. However, its molecular mechanism in retinopathy has not been reported.

Thus, we studied the molecular mechanism of LCN2 in streptozotocin (STZ)-induced rats and HG-induced HRVECs respectively. To our surprise, we found that LCN2 was significantly up-regulated in STZ-induced retinal and HG-induced HRVECs, and that silencing LCN2 could inhibit caspase-1 mediated pyroptosis, and attenuate the progression of DR. Our findings may open up new therapeutic strategies for treating diabetic retinopathy. We present the following article in accordance with the ARRIVE reporting checklist (available at https://atm.amegroups.com/article/view/10.21037/atm-22-2655/rc).

Methods

Cell culture and transfection

HRVECs were purchased from Cell Systems Corporation (UK). HRVECs were cultured at 37 ℃ in a 5% CO_2 incubator in a DDMEM medium containing 10% FBS and 1% penicillin/streptomycin. HRVECs in the control group were treated with 5.5 mM glucose and the HG group was treated with 30 mM glucose. When the cell density reached 70% to 80%, the plasmid of sh-NC or sh-LCN2 was transfected with lipofectamine 3000 according to the protocols.

Animal model

A total of 40 male Sprague Dawley (SD) rats (230±10 g, 8-week-old, specific-pathogen-free) were provided by the Experimental Animal Center of Jilin University and kept in comfortable cages with a humidity of 55%, a light/dark cycle of 12 hours, and a temperature of 22 ℃. In the cages, rats had free access to food and water. Diabetes was induced by intraperitoneal injection of STZ (65 mg/kg) after 1 week acclimation. Rats in the sham group received an equal amount of buffer intraperitoneally. Blood glucose concentration was monitored daily, and fasting blood glucose concentration was higher than 16.7 mmol for a consecutive week, indicating the successful establishment of the diabetes model (18). After 2 months of diabetes induction, the rats were euthanized, and retinal tissue was harvested. The animal experiments in the study were approved by the Animal Ethics Committee of the First Affiliated Hospital of Jiamusi University. Experiments were performed in compliance with national guidelines for the care and use of animals. A protocol was prepared before the study without registration.

Intravitreal adeno-associated virus injection

To make the injection more convenient, the right eyes were given topical treatments with 1% atropine sulfate and 2.5% phenylepinephrine hydrochloride. The sequence of sh-LCN2 or sh-NC was cloned into an adeno-associated virus (AAV2) vector and packaged into AAV by General Biotech. Using a microinjector, 4 μL AAV-NC or AAV-sh-LCN2 was injected into the vitreous cavity of rats. In particular, AAV was injected 2 weeks before induction of diabetes.

Reverse transcription quantitative polymerase chain reaction analysis

The total RNA was extracted with TRIzol reagent (Thermo Fisher Scientific, Waltham, MA, USA) and the SuperScript IV Reverse Transcription Kit (Thermo Fisher, USA) was used to prepare complementary DNA (cDNA) samples. Reverse transcription quantitative polymerase chain reaction (RT-qPCR) analysis was performed to detect the messenger RNA (mRNA) expression of LCN2 using IQ SYBR Green Supermix (Bio-Rad, Hercules, CA, USA). Glyceraldehyde 3-phospahte dehydrogenase (GAPDH) was acted as an endogenous control. The relative expression levels were calculated using the $2^{-\Delta\Delta CT}$ method.

Western blotting assay

Proteins were extracted from HRVECs and retinal tissues using radioimmunoprecipitation assay (RIPA) lysates, and protein concentrations were determined with a bicinchoninic acid (BCA) kit. The protein samples were subjected to sodium dodecyl sulfate polyacrylamide gel electrophoresis (SDS-PAGE) and then transferred to a polyvinylidene fluoride (PVDF) membrane. The PVDF membrane was successively incubated with primary antibody, washed, and then incubated with a secondary antibody. The enhanced chemiluminescence (ECL) approach was used to produce visualization in dark. Image J software (National Institutes of Health, Bethesda, MD, USA) was used to analyze the gray value to evaluate the relative protein expression level. We used GAPDH as the internal control.

Wound healing assay

The migration was detected using a wound healing test. As previously reported (19), the HRVECs were seeded in a 24-well plate, and after the cell confluency reached more than 80%, a pipette tip was used to scrape the surface. The cells were then cultivated for 24 hours, and the scratches were examined under a microscope (Leica, Wetzlar, Germany) to assess cell migratory ability.

Transwell experiment

The HRVECs were inoculated on the top layer of the transwell chamber in serum-free medium, then transferred to the lower chamber of complete medium containing 10% fetal bovine serum (FBS), and placed in a 37 ℃ incubator for 24 hours. The migrated cells were fixed with fixative for 10 minutes and stained with 0.1% crystal violet for 15 minutes. After rinsing with phosphate-buffered saline (PBS), the HRVECs were observed under a microscope and photographed randomly, and analyzed.

Tube formation experiment

Angiogenesis ability was evaluated by tube formation experiments. Briefly (20), HRVECs were inoculated into 48-well plates pre-coated with Matrigel 48 hours after transfection. After incubation in a 37 ℃ incubator for 24 hours, observation was performed under a microscope and photographs were taken. The capillary-like structures were counted and statistically analyzed.

Terminal deoxynucleotidyl transferase (TdT)-mediated dUTP biotin nick end labeling staining

To assess the apoptosis of HRVECs, the media was removed and the cells were rinsed with PBS. The cells were fixed for 30 minutes with immunostaining fixative before being rinsed once with PBS. The immunostaining washing solution was added, and the cells were incubated in an ice bath for 2 minutes. Then, 50 μL terminal deoxynucleotidyl transferase biotin-dUTP nick end labeling (TUNEL) staining reagent was added, and the cells were incubated at 37 ℃ for 60 minutes in the dark, and washed with PBS. For diabetic rats, the paraffin sections were dewaxed and then antigen repaired. Then, the slices were immersed in 3% H_2O_2 solution for 5 minutes and rinsed with PBS. The sections were incubated with immunostaining detergent and TUNEL staining solution. The fluorescence intensity was observed under a fluorescence microscope, and 5 fields were randomly selected for photography and analysis.

Flow cytometry

According to the instructions, FAM-YVAD-FMK (FLICA) and propidium iodide (PI) staining samples were analyzed by flow cytometry to detect pyroptosis (21). Approximately 5,000 HRVECs cells in each sample were analyzed using Accuri™C6 Plus [Becton, Dickinson, and Co. (BD) Biosciences, Franklin Lakes, NJ, USA].

Immunohistochemical (IHC) staining

The retinal tissue was embedded in paraffin, sectioned, and

dewaxed, then hydrated with gradient alcohol and washed with PBS for 3 times. After antigen repair, PBS washing was performed twice and the samples were sealed with 5% bovine serum albumin (BSA) at room temperature for 10 minutes. The sections were incubated with the specific primary antibody at 4 ℃ overnight. After washing with PBS again, the secondary antibody was added and incubated at 37 ℃ for 1 hour. After washing with PBS, 3,3'-diaminobenzidine (DAB) was used for 3 minutes and hematoxylin was applied for re-dyeing for 10–15 seconds. After gradient ethanol dehydration, xylene was applied for 5 minutes to achieve transparency. Finally, the sections were sealed with neutral gum, observed under a microscope, and photographed.

Immunofluorescent staining

As previously reported (22), the prepared HRVECs were sealed with PBS containing 5% BSA for 2 hours. Then, sections were incubated overnight with the diluted primary antibody (caspase-1) at 4 ℃. The next day, HRVECs were rinsed 3 times and incubated at room temperature with fluorescent-labeled secondary antibody for 3 hours. Finally, they were observed and photographed under a fluorescence microscope, and the intensity of fluorescence signal was analyzed by image J software.

Histological analysis

Retinal tissue was fixed with 4% neutral formalin and embedded in paraffin. Sections were stained with hematoxylin and eosin (H&E) as per normal procedure (23). Histopathological changes were analyzed professionally by pathologists who were not previously aware of the groups.

Retinal trypsin digestion assay

Retinal trypsin digestion was detected using the previously reported method (24). Retinal tissue was harvested and incubated in a 0.1-M Tris buffer containing 3% trypsin at 37 ℃ until the medium became cloudy. It was gently shaken to loosen the vessel network, then rinsed and put on glass slides for drying. Retinal vessels were stained with periodic acid-Schiff-hematoxylin and observed and photographed under a light microscopy.

Statistical analysis

The data in the present study were expressed as mean ± SD. The data were statistically analyzed using SPSS 22.0 software (IBM Corp., Armonk, NY, USA). Statistical significance was assessed using Student's *t*-test or one-way analysis of variance (ANOVA). A P value <0.05 was considered statistically significant.

Results

LCN2 is up-regulated in DR tissues HRVECs under HG conditions

First, the mRNA and protein levels of LCN2 in retinal tissues were detected by RT-qPCR and western blot. As shown in *Figure 1A,1B*, we found that compared with the sham group, the mRNA expression and protein expression of LCN2 in the STZ group were up-regulated significantly. Meanwhile, the LCN2 expression in HRVECs cells induced by HG was detected via RT-qPCR and western blot. It was shown (*Figure 1C,1D*) that compared with control group, the mRNA and protein expression of LCN2 were increased obviously in the HG group.

LCN2 regulates diabetes mellitus-induced retinal vascular dysfunction in vivo

To study the effect of LCN2 on DR, AAV-sh-LCN2 was intravitreally injected into STZ-induced rats. The RT-qPCR results (*Figure 2A*) showed that the mRNA expression of LCN2 in retinal tissues was significantly down-regulated after AAV-sh-LCN2 treatment, which was consistent with the protein expression level detected by western blot (*Figure 2B*). The H&E results (*Figure 2C*) showed that the sham group had intact retinal surface, clear structure, and compact arrangement of cells, while the STZ group had disordered tissue structure and obvious proliferation of endothelial cells. Retinal injury was significantly improved in the AAV-sh-LCN2 group. Furthermore, retinal trypsin digestion tests (*Figure 2D*) showed that elevated glucose led to the formation of retinal capillaries. It could be that AAV-sh-LCN2 reduces harmful effects and improves vascular dysfunction to a certain extent. The results showed that sh-LCN2 could attenuate diabetes mellitus-induced retinal vascular dysfunction *in vivo*.

LCN2 regulates diabetes mellitus-induced pyroptosis in vivo

To further study the regulatory mechanism of LCN2 in DR, TUNEL staining (*Figure 3A*) was used to detect

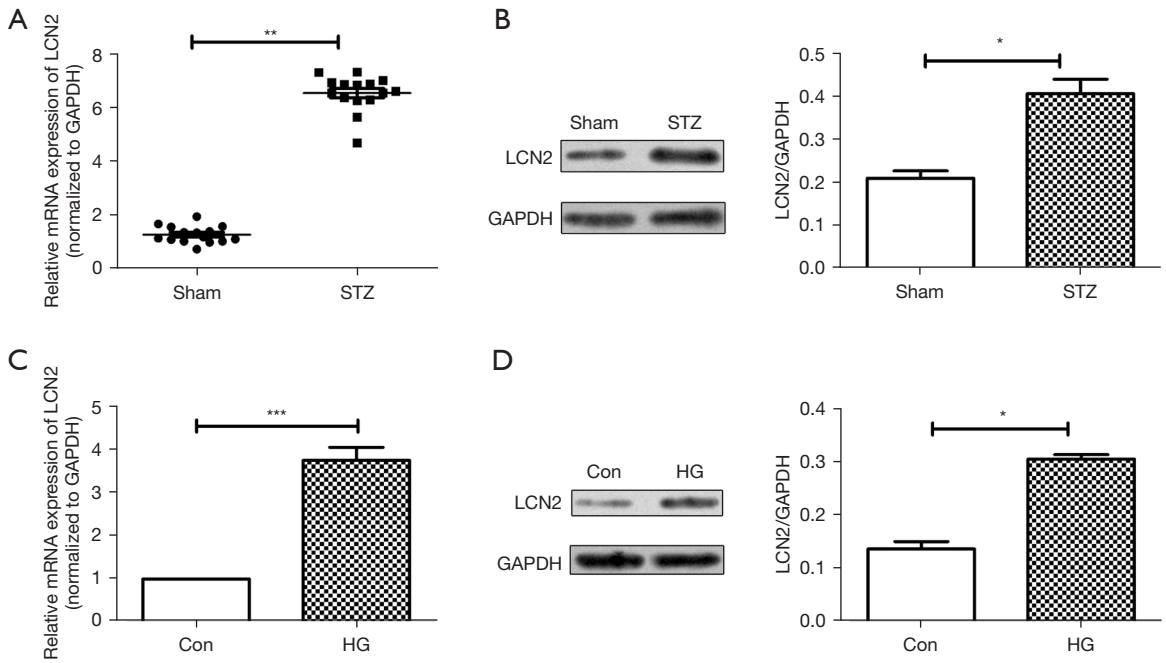

Figure 1 LCN2 is up-regulated in diabetic retinopathy tissues and HG-induced HRVECs. RT-qPCR analysis (A) and western blot (B) were used to detect the mRNA expression of LCN2 in diabetic retinopathy tissues. RT-qPCR (C) and western blot (D) were performed to detect the levels of LCN2 in HG-induced HRVECs. The data were expressed as mean ± SD, n=3. *P<0.05, **P<0.01, *vs.* sham/con group. ***P<0.001. STZ, streptozotocin; HG, high glucose; HRVECs, human retinal vascular endothelial cells; RT-qPCR, reverse transcription quantitative polymerase chain reaction; HG, high glucose; SD, standard deviation.

apoptosis. We found that the TUNEL positive cells in STZ group were increased significantly compared with those in the sham group. When compared with STZ + AA-NC group, the TUNEL positive cells were reduced. The result of western blot (*Figure 3B*) showed that compared with sham group, the expressions of caspase-1, gasdermin D (GSDMD), IL-1β, and NOD-, LRR- and pyrin domain-containing protein (NLRP3) in the STZ group were increased significantly. After intravitreal injection treatment, the expressions of caspase-1, GSDMD, IL-1β, and NLRP3 were down-regulated obviously. Besides, IHC staining result (*Figure 3C*) revealed that the positive signal of caspase-1 was significantly increased in the STZ group and significantly decreased in the AAV-sh-LCN2 group. It is well known that caspase-1 is a potential marker molecule of pyroptosis, and we speculated that sh-LCN2 might affect pyroptosis and alleviate the progression of DR.

LCN2 regulates endothelial cell function under HG conditions in vitro

In addition, the effect of LCN2 on HRVECs cell function *in vitro* was studied. The results of RT-qPCR and western blot results (*Figure 4A,4B*) confirmed the success of sh-LCN2 transfection. Vascular endothelial cell migration and angiogenesis are key factors in the progression of DR. Wound healing and Transwell experiment (*Figure 4C,4D*) showed that the migration of HRVECs under HG conditions was significantly enhanced, while the migration of HRVECs was significantly decreased in the sh-LCN2 group compared with HG + NC group. According to the tube formation experiment (*Figure 4E*), we found that compared with control group, the angiogenesis in the HG group was significantly increased. The angiogenesis in HG + sh-LCN2 group was reduced obviously compared with HG + NC group. Taken together, it suggested sh-LCN2 significantly inhibited the migration and angiogenesis in HG-induced HRVECs.

Down-regulation of LCN2 significantly suppress HG-induced pyroptosis in HRVECs

Next, the effect of LCN2 on pyroptosis of HRVECs cells induced by HG was studied *in vitro*. The results (*Figure 5A*)

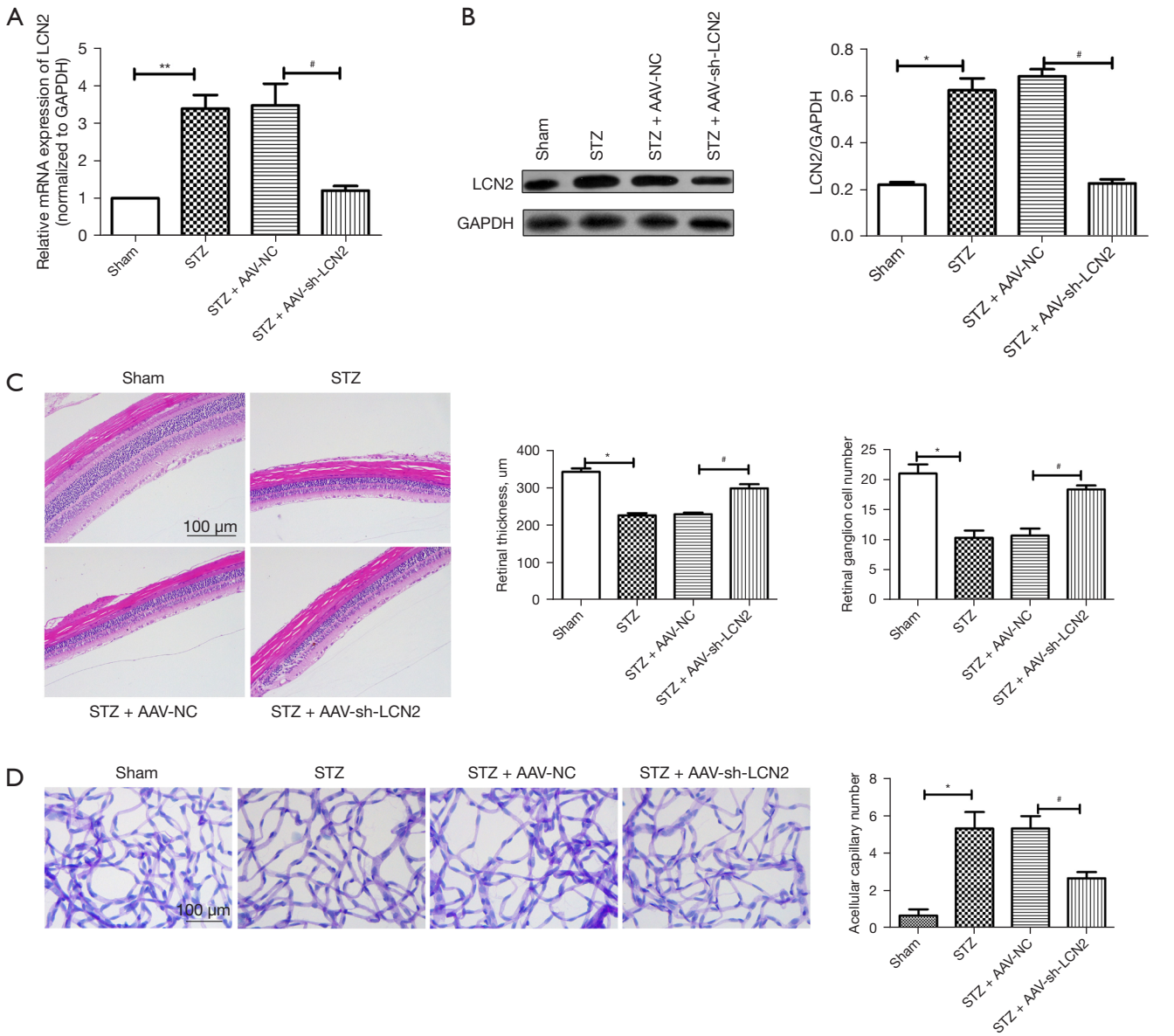

Figure 2 LCN2 regulates diabetes mellitus-induced retinal vascular dysfunction *in vivo*. RT-qPCR analysis (A) and western blot (B) were used to detect the mRNA expressions and protein expression of LCN2. (C) H&E staining was performed to observe the pathological changes (×200). (D) Pericyte degeneration and acellular capillaries were detected by retinal trypsin digestion (×200). The data were expressed as mean ± SD, n=3. *P<0.05, **P<0.01, *vs.* sham group; #P<0.05, *vs.* STZ + AAV-NC group. RT-qPCR, reverse transcription quantitative polymerase chain reaction; mRNA, messenger RNA; H&E, hematoxylin and eosin; STZ, streptozotocin; AAV, adeno-associated virus; SD, standard deviation.

of flow cytometry showed that compared with HG + NC group, the pyroptosis in HG + sh-LCN2 group was reduced significantly. The results of TUNEL staining (*Figure 5B*) revealed that compared with HG + NC group, the apoptosis in HG + sh-LCN2 group was reduced significantly. Western blot results (*Figure 5C*) showed that sh-LCN2 significantly down-regulated the expression levels of caspase-1, GSDMD, IL-1β, and NLRP3 in HRVECs induced by HG. Furthermore, immunofluorescence staining results (*Figure 5D*) showed that compared with the control group,

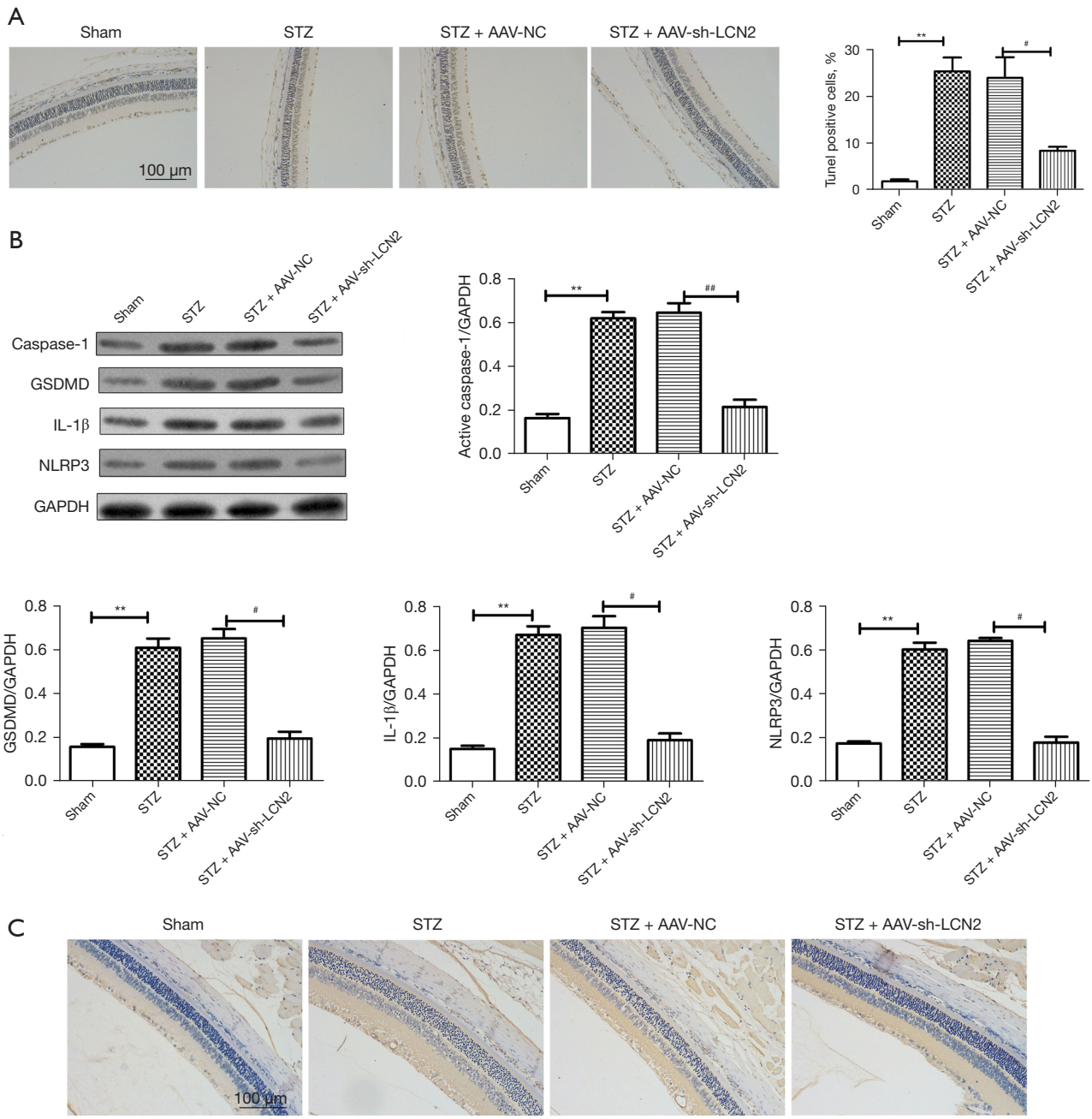

Figure 3 LCN2 regulates diabetes mellitus-induced pyroptosis *in vivo*. (A) TUNEL staining was used to detect the apoptosis (×200). (B) The protein expressions of caspase-1, GSDMD, IL-1β and NLRP3 in retinal tissue were evaluated by western blotting assay. (C) The expression of caspase-1 was detected by IHC staining (×200). The data were expressed as mean ± SD, n=3. **P<0.01, *vs.* sham group; #P<0.05, ##P<0.01, *vs.* STZ + AAV-NC group. GSDMD, gasdermin D; IL-1β, interleukin-1β; NLRP3, NOD-, LRR- and pyrin domain-containing protein; SD, standard deviation; IHC, immunohistochemical; STZ, streptozotocin; AAV, adeno-associated virus.

the caspase-1 signal was significantly enhanced in HG group. The caspase-1 signal in HG + sh-LCN2 group was reduced obviously compared with HG + NC group.

These results confirmed that down-regulation of LCN2 could significantly suppress HG-induced pyroptosis in HRVECs.

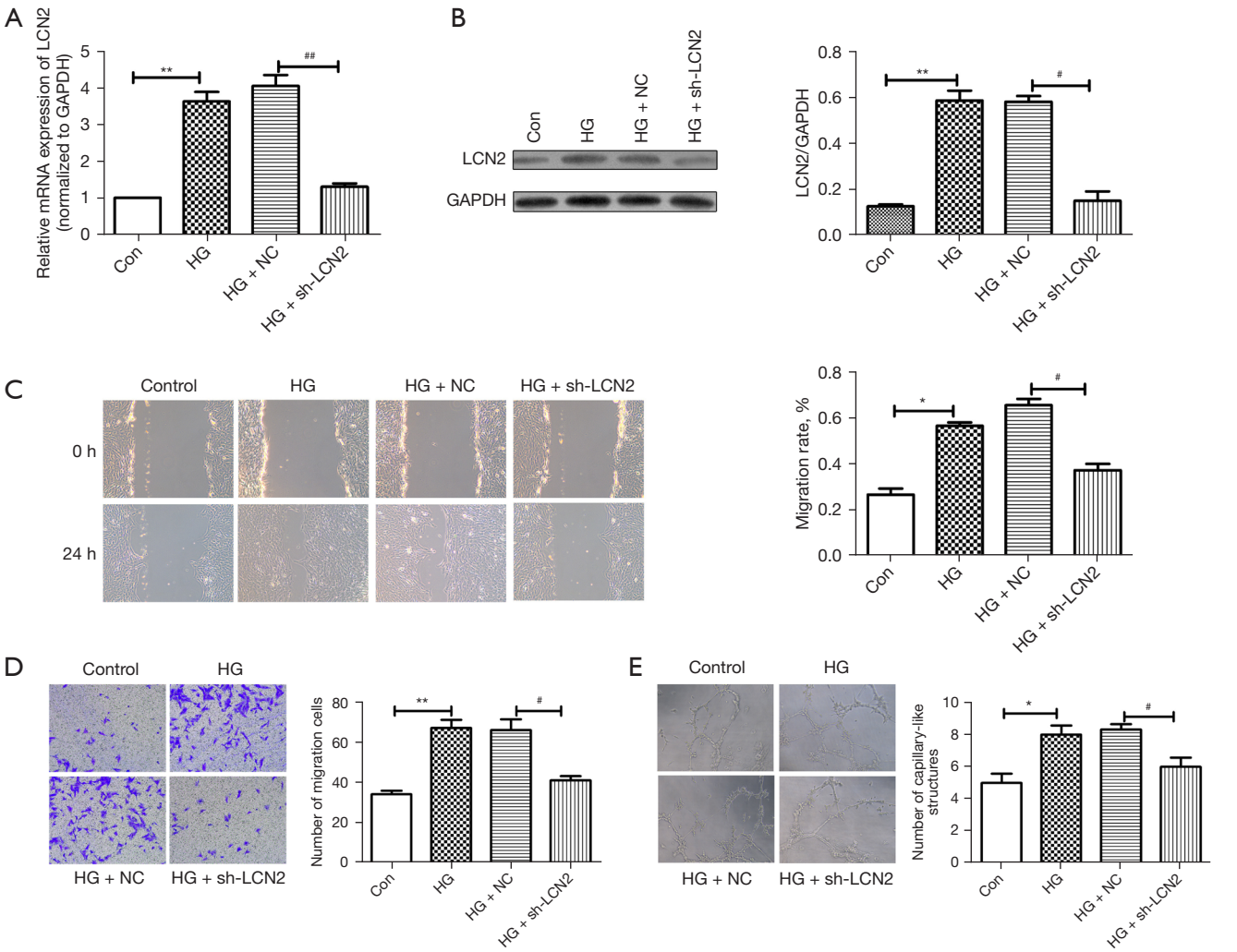

Figure 4 LCN2 regulates endothelial cell function under HG conditions *in vitro*. (A) RT-qPCR analysis was used to detect the mRNA expressions of LCN2 in HRVECs. (B) Western blot was used to detect the protein expression of LCN2 in HRVECs. (C) Wound healing assay was performed to detect the migration (×100). (D) Transwell experiment was used to detect the invasion (×100). (E) Tube formation assay was performed to assess the ability of angiogenesis (×100). The data were expressed as mean ± SD, n=3. *P<0.05, **P<0.01, *vs.* Con group; #P<0.05, ##P<0.01, *vs.* HG + NC group. HG, high glucose; HRVECs, human retinal vascular endothelial cells; SD, standard deviation.

Caspase-1 inhibitor represses HG-induced pyroptosis in HRVECs

To further confirm whether caspase-1 is involved in pyroptosis in HRVECs induced by HG, after VX-765 (caspase-1 inhibitor) treatment, western blotting assay, flow cytometry, and immunofluorescence assay were used to detect the changes of HG-induced pyroptosis in HRVECs. Western blot results (*Figure 6A*) showed that VX-765 could significantly down-regulate the expressions of caspase-1, GSDMD, IL-1β, and NLRP3 induced by HG. Similarly, flow cytometry results (*Figure 6B*) also showed that VX-765 significantly inhibited HG-induced pyroptosis in HRVECs. Then, the expression of caspase-1 was analyzed by immunofluorescence staining. As shown in *Figure 6C*, we found that the positive signal of caspase-1 was significantly stronger in the HG group, and decreased obviously after VX-765 treatment. To sum up, we confirmed that caspase-1 inhibitor inhibited HG-induced pyroptosis in HRVECs.

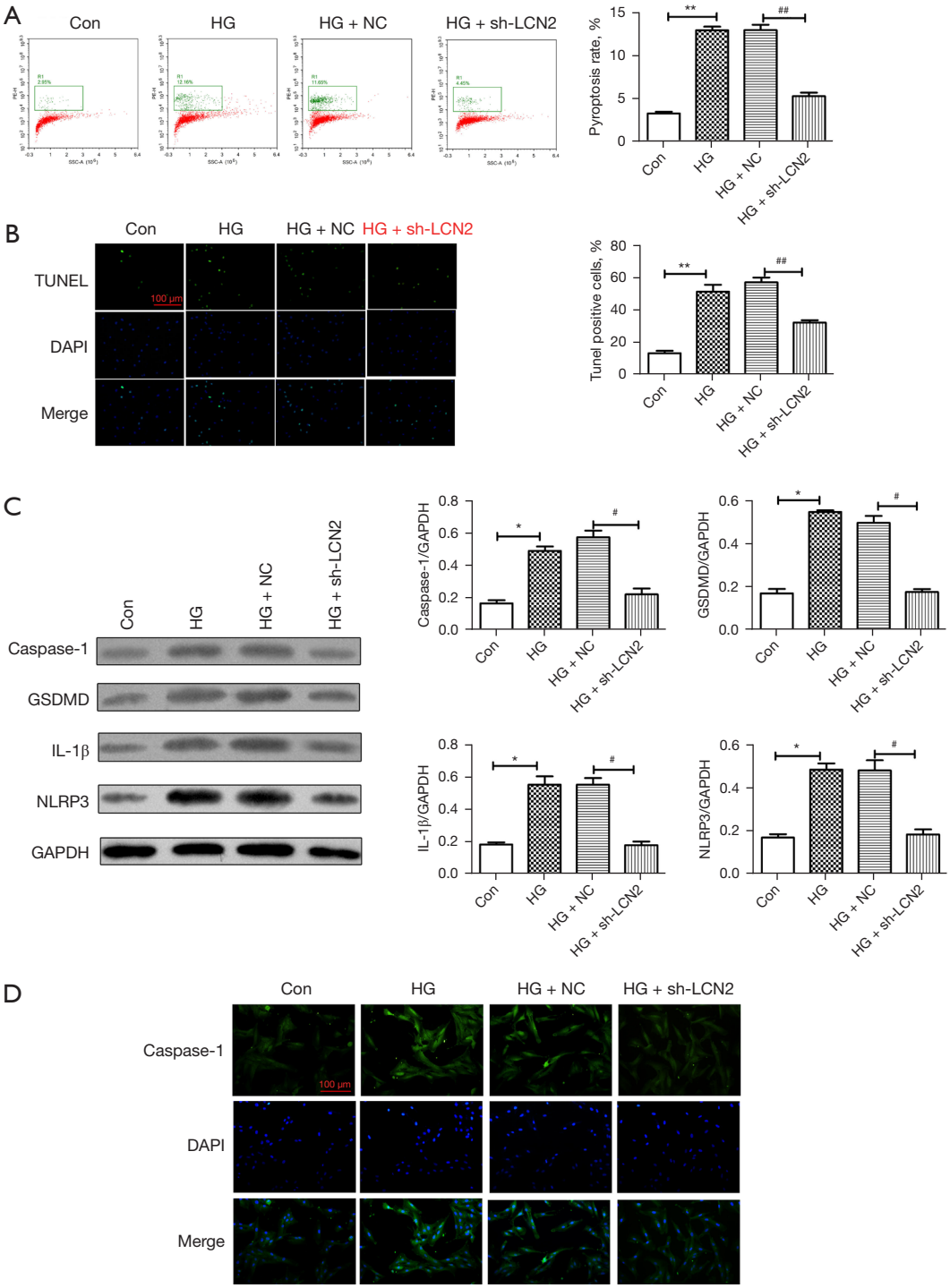

Figure 5 Down-regulation of LCN2 significantly promotes HG-induced pyroptosis in HRVECs. (A) Pyroptosis was detected by flow cytometry. (B) TUNEL staining was used to detect the apoptosis (×100). (C) Western blot was used to detect the protein expressions of casapse-1, GSDMD, IL-1β, NLRP3 in different groups. (D) The caspase-1 expression was detected by immunofluorescence staining (×100). The data were expressed as mean ± SD, n=3. *P<0.05, **P<0.01, *vs.* Con group; #P<0.05, ##P<0.01, *vs.* HG + NC group. HRVECs, human retinal vascular endothelial cells; SD, standard deviation; GSDMD, gasdermin D; IL-1β, interleukin-1β; NLRP3, NOD-, LRR- and pyrin domain-containing protein; TUNEL, terminal deoxynucleotidyl transferase biotin-dUTP nick end labeling.

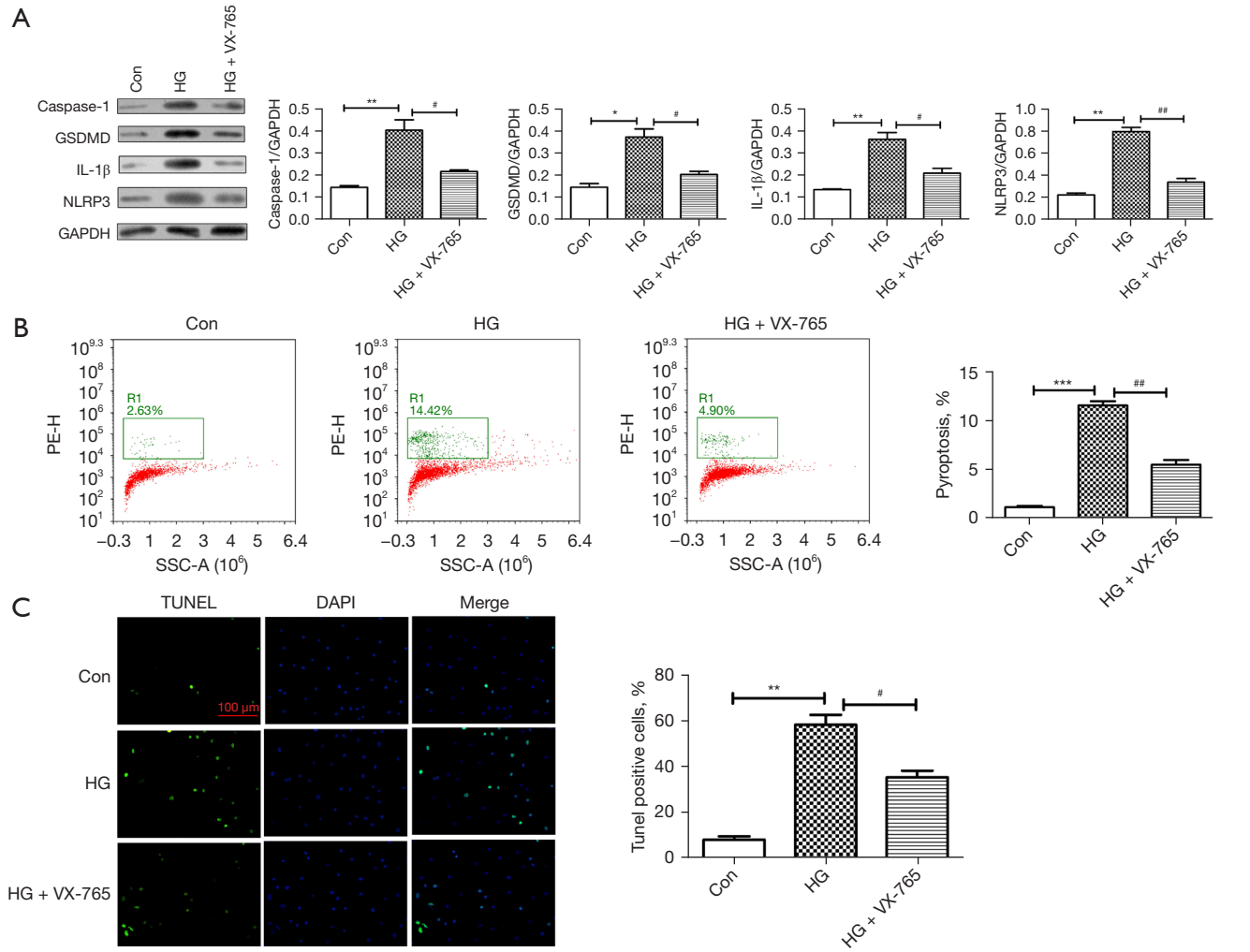

Figure 6 Caspase-1 inhibitor represses HG-induced pyroptosis in HRVECs. (A) Western blot was used to detect the expressions of caspase-1, GSDMD, IL-1β, and NLRP3 in different groups. (B) Pyroptosis was assessed by flow cytometry. (C) TUNEL staining was used to detect the apoptosis (×100). The data were expressed as mean ± SD, n=3. *P<0.05, **P<0.01, ***P<0.001, *vs.* Con group; #P<0.05, ##P<0.01, *vs.* HG group. HG, high glucose; HRVECs, human retinal vascular endothelial cells; GSDMD, gasdermin D; IL-1β, interleukin-1β; NLRP3, NOD-, LRR- and pyrin domain-containing protein; SD, standard deviation.

Discussion

As one of the most serious microangiopathy complications of diabetes mellitus, DR seriously threatens the vision of patients and may cause blindness (25). It is mainly characterized by dysfunction of retinal vascular endothelial cells in HG conditions. The existing treatment strategy is mainly blood glucose control and prevention, but treatment methods are lacking. Our study focused on the improvement of retinal vascular endothelial cell function by inhibiting pyroptosis. We found that LCN2 was significantly up-regulated in DR tissues and HG-induced HRVECs. Silencing of LCN2 could effectively inhibit caspase-1 dependent pyroptosis and improve retinal vascular endothelial cell dysfunction.

The potential molecular mechanism of pyroptosis of retinal vascular endothelial cells has attracted mounting attention from ophthalmic clinicians (26). It has been reported that hyperglycemia can induce GSDMD-mediated pyroptosis and promote endothelial cell dysfunction in DR (27). A HG environment promotes stimulation of the NLRP3-caspase-1-GSDMD signaling axis, which further induces the formation of pores in the plasma membrane

of HRVECs, further promotes the secretion of IL-1β, and aggravates cell loss. In addition, studies (28,29) have shown that in STZ-induced diabetic rat models, increased NLRP3 expression promotes caspase-1 expression and activation of the nuclear factor (NF)-κB signaling pathway, initiating the initial pathological process of DR. Gu *et al.* (30) found that down-regulation of miR-590-3p triggered NOX4/ROS/TXNIP/NLRP3 signaling through IL-1β-mediated positive feedback loops, thereby promoting pyroptosis. Our study found that the expression of LCN2 was significantly up-regulated in DR tissues and endothelial cells induced by HG. Our study found that the pyroptosis-related genes were significantly up-regulated in diabetic retinopathy, including caspase-1, GSDMD, IL-1β and NLRP3. After transfection with sh-LCN2, we found that sh-LCN2 significantly down-regulated the protein expression of the GSDMD/caspase-1/NLRP3 signaling axis. In addition, flow cytometry results suggested that LCN2 silencing could significantly inhibit pyroptosis induced by HG. Interestingly, flow cytometry results suggested that LCN2 silencing could significantly inhibit pyroptosis induced by HG. We hypothesized that LCN2 may be involved in pyroptosis induced by HG and promote DR.

It has been reported that LCN2 is expressed in a variety of cells and organs and is mainly involved in inflammatory response and metabolic regulation (31). The secretion of LCN2 is mainly caused by infection, injury, and metabolic disorder (32), which is consistent with our study. We also confirmed that LCN2 is highly expressed in DR. Secretion of LCN2 interacts with inflammasome regulation, and NLRP3 triggers selective attenuating of LCN2 expression in NLRS-mediated mouse macrophages, slowing down the inflammatory response (32). We demonstrated that LCN2 silencing significantly inhibited NLRP3/caspase-1 mediated pyroptosis. In addition, *in vitro* experiments revealed that LCN2 silencing inhibits vascular endothelial cell migration and angiogenesis, suggesting that LCN2 silencing significantly improves vascular endothelial cell function. *In vivo* experiments suggested that AAV-sh-LCN2 could relieve retinal damage, which may be related to the inhibition caspase-1-dependent pyroptosis.

In conclusion, we found that LCN2 silencing can improve vascular endothelial cell dysfunction and reduce DR. Our findings indicate that inhibition of pyroptosis may be a new therapeutic direction for DR, in which LCN2 may be a new target molecule. In the future, we need to further determine the molecular mechanism of LCN2 regulating pyroptosis via *in vivo* experiments, which may provide a solid theoretical basis for clinical research and potential drug development.

Acknowledgments

We are grateful to all participants for their contributions to the present study.
Funding: The study was funded by 2021 Heilongjiang Provincial Health and Health Commission Research Project (No. 20210707020086).

Footnote

Reporting Checklist: The authors have completed the ARRIVE reporting checklist. Available at https://atm.amegroups.com/article/view/10.21037/atm-22-2655/rc

Data Sharing Statement: Available at https://atm.amegroups.com/article/view/10.21037/atm-22-2655/dss

Conflicts of Interest: All authors have completed the ICMJE uniform disclosure form (available at https://atm.amegroups.com/article/view/10.21037/atm-22-2655/coif). The authors have no conflicts of interest to declare.

Ethical Statement: The authors are accountable for all aspects of the work in ensuring that questions related to the accuracy or integrity of any part of the work are appropriately investigated and resolved. The animal experiments in the study were approved by the Animal Ethics Committee of the First Affiliated Hospital of Jiamusi University. Experiments were performed in compliance with national guidelines for the care and use of animals.

References

1. Leasher J, Bourne R, Flaxman S, et al. Global Estimates on the Number of People Blind or Visually Impaired by

Diabetic Retinopathy: A Meta-analysis From 1990 to 2010. Diabetes Care 2016;39:1643-9.
2. Bek T. Mitochondrial dysfunction and diabetic retinopathy. Mitochondrion 2017;36:4-6.
3. Zheng Y, He M, Congdon N. The worldwide epidemic of diabetic retinopathy. Indian J Ophthalmol 2012;60:428-31.
4. Robinson R, Srinivasan M, Shanmugam A, et al. Interleukin-6 trans-signaling inhibition prevents oxidative stress in a mouse model of early diabetic retinopathy. Redox Biol 2020;34:101574.
5. Lin W, Feng M, Liu T, et al. Microvascular Changes After Conbercept Intravitreal Injection of PDR With or Without Center-Involved Diabetic Macular Edema Analyzed by OCTA. Front Med (Lausanne) 2022;9:797087.
6. Zhang J, Zhang X, Zou Y, et al. CPSF1 mediates retinal vascular dysfunction in diabetes mellitus via the MAPK/ERK pathway. Arch Physiol Biochem 2022;128:708-15.
7. Costa GN, Vindeirinho J, Cavadas C, et al. Contribution of TNF receptor 1 to retinal neural cell death induced by elevated glucose. Mol Cell Neurosci 2012;50:113-23.
8. Liu X, Zhang Y, Liang H, et al. microRNA-499-3p inhibits proliferation and promotes apoptosis of retinal cells in diabetic retinopathy through activation of the TLR4 signaling pathway by targeting IFNA2. Gene 2020;741:144539.
9. Wang W, Wang Q, Wan D, et al. Histone HIST1H1C/H1.2 regulates autophagy in the development of diabetic retinopathy. Autophagy 2017;13:941-54.
10. Wang X, Li H, Li W, et al. The role of Caspase-1/GSDMD-mediated pyroptosis in Taxol-induced cell death and a Taxol-resistant phenotype in nasopharyngeal carcinoma regulated by autophagy. Cell Biol Toxicol 2020;36:437-57.
11. Hu Y, Xue J, Yang Y, et al. Lipocalin 2 Upregulation Protects Hepatocytes from IL1-β-Induced Stress. Cell Physiol Biochem 2015;36:753-62.
12. Rahimi S, Roushandeh AM, Ebrahimi A, et al. CRISPR/Cas9-mediated knockout of Lcn2 effectively enhanced CDDP-induced apoptosis and reduced cell migration capacity of PC3 cells. Life Sci 2019;231:116586.
13. Hochmeister S, Engel O, Adzemovic MZ, et al. Lipocalin-2 as an Infection-Related Biomarker to Predict Clinical Outcome in Ischemic Stroke. PLoS One 2016;11:e0154797.
14. Syrjänen S, Naud P, Sarian L, et al. Up-regulation of lipocalin 2 is associated with high-risk human papillomavirus and grade of cervical lesion at baseline but does not predict outcomes of infections or incident cervical intraepithelial neoplasia. Am J Clin Pathol 2010;134:50-9.
15. Kim SL, Min IS, Park YR, et al. Lipocalin 2 inversely regulates TRAIL sensitivity through p38 MAPK-mediated DR5 regulation in colorectal cancer. Int J Oncol 2018;53:2789-99.
16. Santiago-Sánchez GS, Noriega-Rivera R, Hernández-O'Farrill E, et al. Targeting Lipocalin-2 in Inflammatory Breast Cancer Cells with Small Interference RNA and Small Molecule Inhibitors. Int J Mol Sci 2021;22:8581.
17. Xu J, Lv S, Meng W, et al. LCN2 Mediated by IL-17 Affects the Proliferation, Migration, Invasion and Cell Cycle of Gastric Cancer Cells by Targeting SLPI. Cancer Manag Res 2020;12:12841-9.
18. Gong Q, Xie J, Liu Y, et al. Differentially Expressed MicroRNAs in the Development of Early Diabetic Retinopathy. J Diabetes Res 2017;2017:4727942.
19. Yang K, Liu J, Zhang X, et al. H3 Relaxin Alleviates Migration, Apoptosis and Pyroptosis Through P2X7R-Mediated Nucleotide Binding Oligomerization Domain-Like Receptor Protein 3 Inflammasome Activation in Retinopathy Induced by Hyperglycemia. Front Pharmacol 2020;11:603689.
20. Ao H, Liu B, Li H, et al. Egr1 mediates retinal vascular dysfunction in diabetes mellitus via promoting p53 transcription. J Cell Mol Med 2019;23:3345-56.
21. Wen S, Deng F, Li L, et al. VX-765 ameliorates renal injury and fibrosis in diabetes by regulating caspase-1-mediated pyroptosis and inflammation. J Diabetes Investig 2022;13:22-33.
22. Adams DL, Adams DK, Stefansson S, et al. Mitosis in circulating tumor cells stratifies highly aggressive breast carcinomas. Breast Cancer Res 2016;18:44.
23. Zhang MY, Zhu L, Zheng X, et al. TGR5 Activation Ameliorates Mitochondrial Homeostasis via Regulating the PKCδ/Drp1-HK2 Signaling in Diabetic Retinopathy. Front Cell Dev Biol 2022;9:759421.
24. Shan K, Liu C, Liu BH, et al. Circular Noncoding RNA HIPK3 Mediates Retinal Vascular Dysfunction in Diabetes Mellitus. Circulation 2017;136:1629-42.
25. Tonade D, Kern TS. Photoreceptor cells and RPE contribute to the development of diabetic retinopathy. Prog Retin Eye Res 2021;83:100919.
26. Yu X, Ma X, Lin W, et al. Long noncoding RNA MIAT regulates primary human retinal pericyte pyroptosis by modulating miR-342-3p targeting of CASP1 in diabetic retinopathy. Exp Eye Res 2021;202:108300.
27. Huang L, You J, Yao Y, et al. High glucose induces pyroptosis of retinal microglia through NLPR3

inflammasome signaling. Arq Bras Oftalmol 2021;84:67-73.
28. Raman KS, Matsubara JA. Dysregulation of the NLRP3 Inflammasome in Diabetic Retinopathy and Potential Therapeutic Targets. Ocul Immunol Inflamm 2022;30:470-8.
29. Du J, Wang Y, Tu Y, et al. A prodrug of epigallocatechin-3-gallate alleviates high glucose-induced pro-angiogenic factor production by inhibiting the ROS/TXNIP/NLRP3 inflammasome axis in retinal Müller cells. Exp Eye Res 2020;196:108065.
30. Gu C, Draga D, Zhou C, et al. miR-590-3p Inhibits Pyroptosis in Diabetic Retinopathy by Targeting NLRP1 and Inactivating the NOX4 Signaling Pathway. Invest Ophthalmol Vis Sci 2019;60:4215-23.
31. Guo H, Jin D, Chen X. Lipocalin 2 is a regulator of macrophage polarization and NF-κB/STAT3 pathway activation. Mol Endocrinol 2014;28:1616-28.
32. Ahn H, Lee G, Kim J, et al. NLRP3 Triggers Attenuate Lipocalin-2 Expression Independent with Inflammasome Activation. Cells 2021;10:1660.

(English Language Editor: J. Jones)

Cite this article as: Su X, Zhou P, Qi Y. Down-regulation of LCN2 attenuates retinal vascular dysfunction and caspase-1-mediated pyroptosis in diabetes mellitus. Ann Transl Med 2022;10(12):695. doi: 10.21037/atm-22-2655

